Image auto-zoom technology for AFM automation*

LIU Wen-liang(刘文良), QIAN Jian-qiang(钱建强) , and LI Yuan(李渊)**
School of Science, Beijing University of Aeronautics and Astronautics, Beijing 100083, China

(Received 16 November 2008)

For the case of atomic force microscope (AFM) automation, we extract the most valuable sub-region of a given AFM image automatically for succeeding scanning to get the higher resolution of interesting region. Two objective functions are summarized based on the analysis of evaluation of the information of a sub-region, and corresponding algorithm principles based on standard deviation and Discrete Cosine Transform (DCT) compression are determined from math. Algorithm realizations are analyzed and two select patterns of sub-region: fixed grid mode and sub-region walk mode are compared. To speed up the algorithm of DCT compression which is too slow to practical applied, a new algorithm is proposed based on analysis of DCT's block computing feature, and it can perform hundreds times faster than original. Implementation result of the algorithms proves that this technology can be applied to the AFM automatic operation. Finally the difference between the two objective functions is discussed with detail computations.

Document code: A **Article ID:** 1673-1905(2009)02-0143-4
DOI 10.1007/s11801-009-8163-2

To develop scientific experiments in extreme circumstances, many traditional manually operation instruments progressively realize automation and achieve good results. In the field of atomic force microscope (AFM), the first AFM on Mars [1] which was boarded on "Phoenix" explorer launched by NASA, and it realized sampling and scanning automatically in the remote Mars.

The objective of this article is to extract the most valuable sub-region automatically for the next scanning according to the obtained AFM image.

First we need to analyze the criterions to identify one sub-region which is more valuable for scanning than others.

From the dust image in Fig.1 (a) [2], one can easy to reach the following judgment: region 2 and 3 have more information than region 1 and 4, because region 1 and 4 is flat, region 2 and 3 have many particles, that is to say, these regions have larger height variation. Analysis of a large number of AFM images shows that regions with large height variation have more information.

The second case is much more complicated, as shown in Fig.1(b) [3], the region 1 which represents the E. coli body has the largest height variation, but people concert more about the region 2 and 3 which represent the complicate flagellum. Difference between region 2 or 3 and region 1 is that: the former have abundant details, the latter is lack of details. Analysis of a large number of similar images shows that regions with abundant details have more information.

The goal of this research can be described as the following two points:

1) Select the sub-region with the largest height variation automatically for a given AFM image.

2) Select the sub-region with the most abundant details automatically for a given AFM image.

The analysis of E. coli image shows that the results of this two target may be different sometimes, and the search strategy is depended on the specific application.

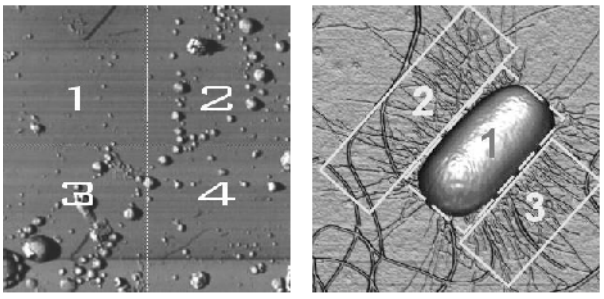

(a) AFM image of dust (b) AFM image of E.coli

Fig.1 Typical AFM image

For the first case, we should calculate the standard deviation (STDEV) of the sub-region from mathematics consideration. Standard deviation reflects the discrete degree of a data set. The mathematical expression is as follows:

* This work has been supported by the National High Technology Research and Development Program of China (Grant No. 2007AA122128)

** E-mail: qianjq@buaa.edu.cn.

$$\sigma = \sqrt{\frac{\sum_{i=1}^{n}(s_i - \bar{s})^2}{n}} \quad . \tag{1}$$

For the second case, an image with abundant details must be an image with complicated information, shown as less information correlation, from the perspective of compression; it must have smaller compression radio. There are many kinds of transform for compression in mathematics [4,5]; the discrete cosine transform (DCT) is utilized in this article [6-8].

For an image with $N \times N$ sampling points, the basic DCT and IDCT formulate are

$$F(u,v) = \frac{2}{N}\sum_{i=0}^{N-1}\sum_{j=0}^{N-1} f(i,j)\cos\frac{(2i+1)u\pi}{2N}\cos\frac{(2j+1)u\pi}{2N}, \tag{2}$$

$$f(i,j) = \frac{\sqrt{2}}{N}\sum_{u=0}^{N-1}\sum_{v=0}^{N-1} F(u,v)\cos\frac{(2i+1)u\pi}{2N}\cos\frac{(2j+1)u\pi}{2N}, \tag{3}$$

For two-dimensional image, compression is realized by using Quantization Table[7] to quantize the DCT transform matrix. The compression radio is defined as CMPR=(P_{Zero}/ P_{Total})× 100%, and P_{zero} is the zero number of the data set after DCT and quantization, P_{Total} is the total pixel number of the original data set.

Through the above analysis, the two criterions can be summed up in two objective functions:

$$f_{T1} = \text{Maxmum}\left[\text{standard deviation}\left(\text{sub - region}\right)\right], \tag{4}$$

$$f_{T2} = \text{Minimum}[\text{CMPR}[\text{zero statistic}[\text{Quantized}[\text{DCT}(\text{sub}-\text{region})]]]]. \tag{5}$$

There are two kinds of selecting patterns of sub-region, the first is fixed grid mode, and the second is sub-region walk mode, shown in Fig.2. From the perspective of computational complexity, the former is much less than the latter. But from the perspective of final result, the former has obvious defect, unless the selected region just falls within the fixed grid, or it will cause serious "region loss", and the probability of this situation is very small. So, sub-region walk mode is utilized in this article.

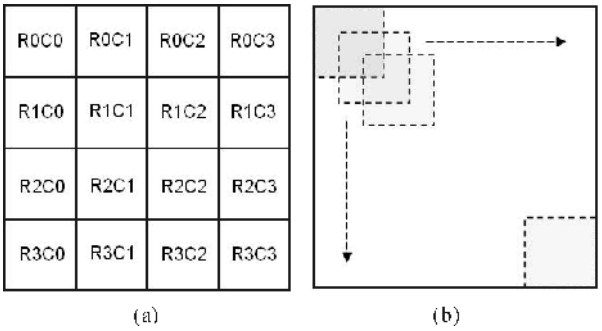

Fig.2 Schematic diagram of fixed grid mode (a) and region walk mode (b)

Let the original image size as $N \times N$, the selected region size as $M \times M$, the walk step is S, then the number of sub-region needed to be analyzed is: $CN = \left((N-M)/S+1\right)^2$, it shows that solving the problem of high computation complexity of sub-region walk mode depends on such two points: first, sub-region size should not be too small; second, the walk step should be increased. And increasing walk step also means increasing the inaccuracy.

Fig.3 shows the result of this two algorithms applied to the 512×512 dust image using sub-region walk mode. The selected sub-region sizes are 256 × 256 and 128 × 128, respectively, and the walk step is 8. The result is good because it is in accordance with the artificial evaluation.

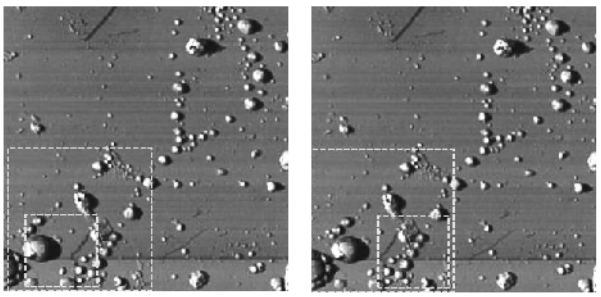

Fig.3 Result of region selecting of the dust AFM image

Tab.1 shows the calculation details of Fig.3, which includes selected region's origin in original image coordinate, time consumption and value of objective function. The origin of the image is top left corner, the positive direction for the x- axis is right, and down for y-axis.

Tab.1 Calculation parameters and results of Fig.3

Size	256 × 256 (Step=32)			256 × 256 (Step=16)		
	Origin	Time/s	Result	Origin	Time/s	Result
STDEV	32,224	0.4218	25.55	16,240	1.6718	27.30
DCT	96,224	4.3125	89.30%	96,240	18.468	88.75%
Size	128 × 128 (Step=16)			128 × 128 (Step=8)		
	Origin	Time/s	Result	Origin	Time/s	Result
STDEV	32,368	0.9687	35.56	40,376	3.7968	36.55
DCT	96,368	9.3125	85.84%	120,376	37.453	85.24%

The direct DCT compression algorithm is too slow, shown in Tab.1, So it can't be applied practically considering the drift of tip when AFM relocation. A new algorithm is proposed in this section to make it 100 times faster.

The root cause of this problem is that too many DCTs are done in the process.

The amount of sub-region that need to be analyzed is certain when original image size, sub-region size and step are given. The thinking to reduce DCT is to make one DCT for many sub-region compression radio calculation.

First a special situation is analysed, original image size is 512 × 512, sub-region size is 128 × 128, the step is 8. The sub-region that need to be analyzed can be treated as a rectangle move above the original image with fixed size, which is represented by the origin in the original image coordinate:

$$\begin{matrix} (0,0) & (0,8) & (0,16) & \cdots & (0,384) \\ (8,0) & (8,8) & & & \vdots \\ (16,0) & & & & \vdots \\ \vdots & & & & \\ (384,0) & \cdots & \cdots & & (384,384) \end{matrix}$$

Because the DCT calculation is based on 8×8 sub-block, if the dataset of the original image after DCT and quantization is $QT_f[512, 512]$, the datasets of (0,0) and (0,8) sub-region after DCT and quantization are $QT_f[0,0]$ and $QT_f[0, 8]$, then $QT_f[0,0]$ and $QT_f[0,8]$ are just the sub-blocks of $QT_f[512, 512]$, they have the same value. In the same way, all $QT_f[8n, 8n]$ $(0 \leqslant n \leqslant 48)$ are sub-block of $QT_f[512, 512]$, so only one DCT is necessary for all 49 × 49 sub-regions, which reduces the computation complexity to $1/(49 \times 49)$.

Next on more general situation, step is 1. The sizes of image and sub-region are the same as the above. At this time $QT_f(x, y)$ $(x \neq 8n, y \neq 8m)$is not the sub-block of $QT_f[512, 512]$ anymore, the sub-region is analysed again as follows.

$$\begin{matrix} (0,0) & (0,1) & (0,2) & \cdots & (0,8) & \cdots & (0,384) \\ (1,0) & & & & & & \vdots \\ (2,0) & & & & & & \vdots \\ \vdots & & & & & & \vdots \\ (8,0) & & & & & & \vdots \\ \vdots & & & & & & \vdots \\ (384,0) & \cdots & \cdots & \cdots & \cdots & \cdots & (384,384) \end{matrix}$$

The more sample way of expressions is as follows.

$$\begin{matrix} 0 & 1 & 2 & \cdots & 8 & \cdots & 384 \\ 1 & & & & & & \vdots \\ 2 & & & & & & \vdots \\ \vdots & & & & & & \vdots \\ 8 & & & & & & \vdots \\ \vdots & & & & & & \vdots \\ 384 & \cdots & \cdots & \cdots & \cdots & \cdots & \end{matrix}$$

Considering one dimension, for example *x*-axis, we can divide 0 to 384 in 8 groups as follow:

$$\begin{matrix} group\_1 & 0 & 8 & 16 & \cdots & 376 & 384 & & \\ group\_2 & & 1 & 9 & 17 & \cdots & 377 & & \\ group\_3 & & & 2 & 10 & 18 & \cdots & 378 & \\ \cdots & & & & \cdots & & & \cdots & \cdots \\ group\_8 & & & & & 7 & 15 & 23 & \cdots & 383 \end{matrix}$$

Then because each group has a step as 8, which meets the condition discussed before, one time DCT and quantization can solve all compression radio for all sub-regions in the group. So, one dimension needs 8 times DCT and quantization, and 64 times for two dimensions. It should be noted that not all 64 sub-regions for DCT have the same size and origin.

Tab.2 shows the efficiency difference between before and after algorithm improvement for analyzing the same Fig.1(a).

Tab.2 Algorithm efficiency comparison before and after improvement

	Sub-region NO.	DCT NO.	Time/s
256 × 256 (step = 8)			
Old	1089	1089	59.953125
New	1089	1	0.312500
128 × 128 (step=8)			
Old	2401	2401	37.453125
New	2401	1	0.234375

It shows clearly that the efficiency of improved algorithm is 150 to 200 times faster than that of the original; it will be much faster when the value of step decreases. This speed is high enough to ignore the drift of the tip and meet the needs of practical application.

Fig.4 and 5 show more results got by applying these two kinds of algorithm to the AFM images with 1/2*N* and 1/4 as the sub-region's size.

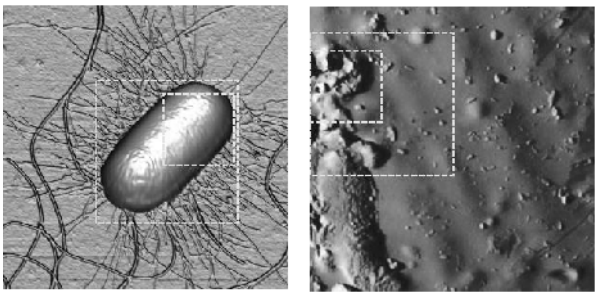

(a) (b)

Fig.4 Result of region selecting based on standard deviation

These results prove the efficiency of two algorithms and the differences between them, which accurately counterparts

the analysis on the first section.

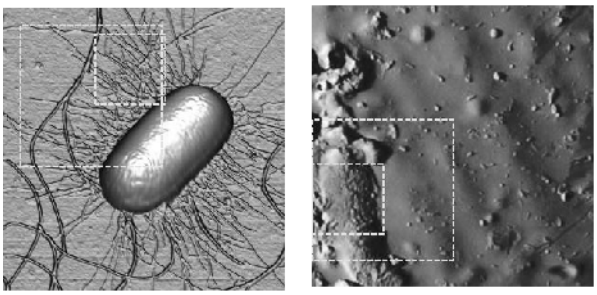

(a) (b)

Fig.5 Result of region selecting based on DCT compression

In summary, in order to extract the most valuable subregion automatically based on the AFM image to get the higher resolution of the interesing region, a corresponding algorithm is proposed and realized. The results show that this method can be applied to the AFM automatic operation.

References

[1] Sebastian Gautsch. Development of An Atomic Force Microscope and Measurement Concepts for Characterizing Martian Dust and Soil Particles [D]. Switzerland, 2002.

[2] M. A. Anderson, W. T. Pike and C.M. Weitz, Microscopy of Analogs for Martian Dust and Soil [DB/OL]. http://mars.jpl.nasa.gov/mgs/sci/fifthconf99/6210.pdf.

[3] Ang Li. Escherichia coli (E. coli) with Pili and Flagella[DB/OL]. http://nanoobjetos.fmc.uam.es/spmage07/imageviewONE.php?id=50

[4] Albert Boggess, Francis J.Narcowich. A First Course in Wavelets with Fourier Analysis [M]. Beijing: Electronic Industry Press, 2004.

[5] Junli Zheng, Qiheng Ying, Weili Yang. Signal and System£ºthe second edition [M]. Beijing: China Higher Education Press, 2000.

[6] International Standards Committee International Standard 10918, American National Standards Institute, New York, 1990.

[7] G.K.Wallace, IEEE Transaction on Consumer Electronics, **38** (1992), 18.

[8] Brian C. Smith, Lawrence A. Rowe. IEEE Computer Graphics & Applications. Volume: **13** (1993), 34.